Progress In Electromagnetics Research C, Vol. 105, 11–21, 2020

Surface Fault Detection in Pipelines Using CSRR Microwave-Based Sensor

Euclides L. Chuma[1, *], Yuzo Iano[2], Sergio Barcelos[1], Luis Ernesto Ynoquio Herrera[1], Laez Barbosa da Fonseca Filho[1], and Rodolfo Cruz[2]

Abstract—This article presents a metamaterial-based microwave sensitive sensor with a complementary split-ring resonator (CSRR) structure for nondestructive surface fault detection in pipelines. The CSRR resonator is etched in the ground plane of a microstrip line and is produced using printed circuit board technology. The novelty of the proposed sensor is its structure that allows it to be directly used for nondestructive fault detection in pipelines, based on frequency and Q factor variations, even for faults under a coating. A measurement setup was used to test the proposed sensor in pipelines of different materials: steel, PVC, and aluminum. The sensor could detect faults of 1 mm. For a hole of 1 mm, the frequency shift was 6.10 MHz in steel, 2.62 MHz in polyvinyl chloride (PVC), and 1.70 MHz in aluminum. In some conditions, the Q-factor shift measurements were 6.72, 5.18, and 7.15 for steel, PVC, and aluminum, respectively. The proposed sensor features high sensitivity, small size, simple design, and easy fabrication.

1. INTRODUCTION

Pipeline transport is the long-distance transportation of different materials such as petroleum, natural gas, and minerals through a system of pipes — a pipeline — typically to a market area for consumption. Pipelines are made from steel or plastic tubes, and various methods are used to protect pipes from impact, abrasion, and corrosion. These methods include polyethylene coating, epoxy coating, concrete coating, imported sand padding, and using padding machines [1].

Pipelines are an economical and safe means of transporting materials to meet the high demands for efficiency and reliability [2]. However, as pipeline transport has become popular in recent decades, critical accidents due to pipeline failures increase [3]. The causes of the failures can be intentional (such as vandalism or terrorism) or unintentional (such as material failure and corrosion) damages [4]. Pipeline failure generally results in environmental pollution and financial losses, particularly when the leakage is not timely detected.

There are several pipeline leak detection methods, which are based on different working principles and approaches [5], and more common methods include the use of acoustic emission [6], fiber optic sensor [7], ground penetration radar [8, 9], negative pressure wave [10], pressure point analysis [11], infrared thermography, and mass-volume balance [12].

This article presents a microwave-based method that involves using a complementary split-ring resonator (CSRR) metamaterial structure that shows a quasi-resonant behavior (in terms of frequency and Q-factor) that varies when the resonator is placed near the object under analysis.

Microwave sensors have gained importance in many research and industrial areas such as the chemical [13–15] and biomedical sectors [16–18] mainly because of their high sensitivity, robustness, and low cost.

Received 2 May 2020, Accepted 9 August 2020, Scheduled 22 August 2020

* Corresponding author: Euclides Lourenço Chuma (euclides.chuma@ieee.org).

[1] Photonics Innovation Institute — iTech, Campinas-SP, Brazil. [2] University of Campinas — UNICAMP, Campinas-SP, Brazil.

In recent years, a new microwave sensing platform using the concept of metamaterials has been introduced [19, 20]. Metamaterials are artificially engineered materials that can manipulate electromagnetic waves, causing the materials to have electromagnetic properties that do not occur or are not readily available in nature [21]. Metamaterials are being studied to find their applications in material sensing in a broad spectral range, including microwaves [22], terahertz [23], and optics [24].

Microwave sensors for crack detection in metallic materials using CSRR have already been studied in other works [25–29]. However, in this work, a microwave sensitive sensor using CSRR geometry and with a new physical structure is reported for the nondestructive detection of faults in pipelines, even for faults under the pipeline coating and with pipelines of different materials: steel, polyvinyl chloride (PVC), and aluminum, and showing good fault detection.

2. THEORETICAL STUDY AND SENSOR DESIGN

The split-ring resonator (SRR) was proposed by Pendry et al. in 1999 [30], and the CSRR was proposed by Falcone et al. in 2004 [31, 32] and can have a circular or square shape [30, 33] with multiple split-ring resonators. Both the SRR and CSRR provide a good, stable frequency response. In our design, a CSRR was used instead of an SRR because the CSRR sensor does not require extra circuit area, making the proposed sensor more compact. To improve the Q-factor of the sensor, multiple split-ring resonators can be used [34].

The equivalent circuit model cell can still be representative in terms of suitable RLC elements by considering the distributed inductances (for CSRR) between adjacent rings [35]. The equivalent circuit model for the squared CSRR cell is shown in Fig. 1 [36].

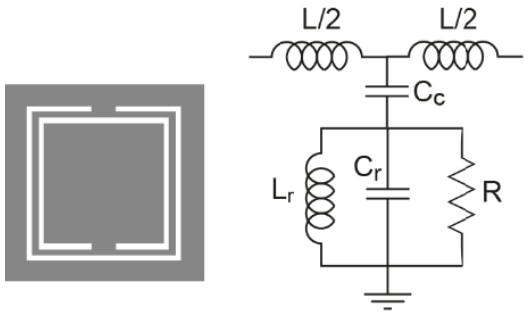

Figure 1. Example of a CSRR and its equivalent circuit model.

The operation of the sensor occurs when a microstrip transmission line is fed by a microwave source. The microstrip line excites the CSRR by inducing a voltage difference between the capacitive plate of CSRR and the ground plane. Consequently, the resonance occurs when the stored electric energy in the C_C and C_r capacitors equals the magnetic energy in the inductive microstrip L_r. During resonance, an electric field is established, making the region near the CSRR sensitive to dielectric changes. Therefore, this region can be used to measure the dielectric properties of materials.

In [25–29], CSRRs were utilized as a sensor to detect surface cracks through changes changes in the reflection coefficient. CSRRs sensors are capable of detecting smaller surface faults such as fatigue cracks, yet the change in standing wave measurement (measured voltage using a detector) is small [27]. The resonant frequency of the circuit model of Fig. 1 can be defined as follows [37]:

$$f_r = \frac{1}{2\pi\sqrt{L_r(C_c + C_r)}} \tag{1}$$

The Q-factor of the resonance is

$$Q = R\sqrt{\frac{C_r + C_C}{L_r}} \tag{2}$$

since the C_r capacitor is affected by the dielectric materials placed near the CSRR center.

The main parts of the proposed sensor are the CSRR on the ground plane and the transmission line on the other side of the board. The CSRR structure and the transmission line must be aligned. Fig. 2 shows the (a) dimensions of the sensor side and (b) the transmission line side, and (c) CSRR details.

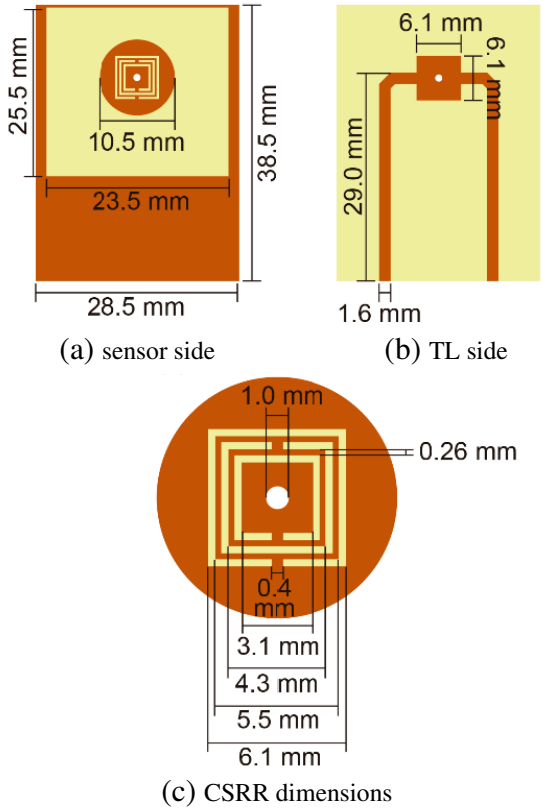

Figure 2. Proposed sensor dimensions of (a) sensor side and (b) transmission line side; (c) details of CSRR.

The new physical structure proposed has an additional dielectric plate with a circular window to maintain constant the distance between the CSSR and the pipeline, in order to avoid differences during the measurements on the surface of the same pipeline. The geometry of the transmission line with the square aligned with the CSRR is also a novelty for microwave pipeline sensors and this physical structure makes the coupling between CSRR and transmission line more sensitive [38].

3. FABRICATION AND MEASUREMENT

The proposed sensor was designed with a Rogers RO3035 substrate with $\varepsilon = 3.5$, $\tan\delta = 0.0015$, and a thickness of 0.75 mm. The CSRR resonant frequency was 2.25 GHz without contact with the pipeline surface, and the dimensions were optimized using the full-wave simulator Ansys HFSS. The simulation of electric field distribution on the surface of the proposed sensor at the resonant frequency is illustrated in the Fig. 3.

The measured and simulated S_{21} of the proposed sensor without pipeline contact are shown in Fig. 4. There is a good agreement between the simulated and measured values, and the differences are probably due to factors that were not considered in the simulation, such as the connectors for example.

A prototype has been fabricated using the photolithography process. Fig. 5 shows the proposed sensor prototype: the (a) sensor side and (b) transmission side with SMA connectors.

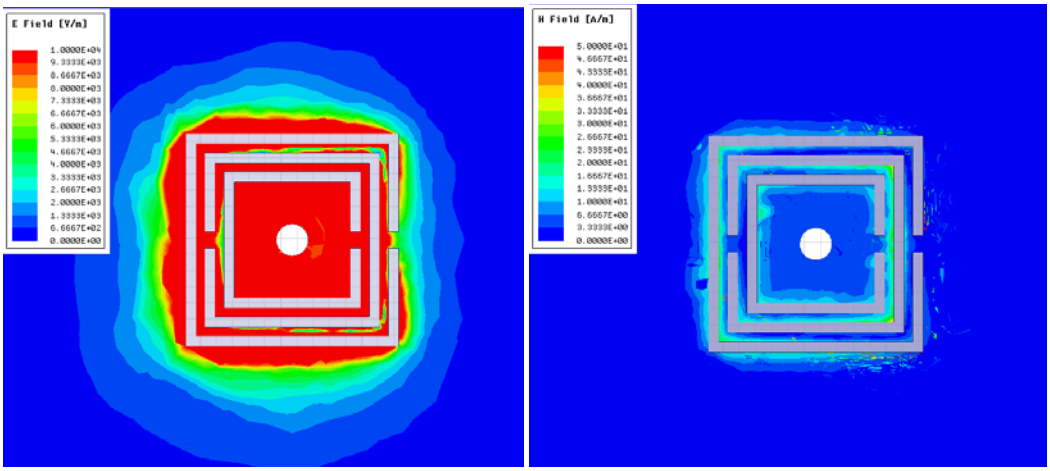

Figure 3. Simulated E field and H field on the surface of the proposed sensor.

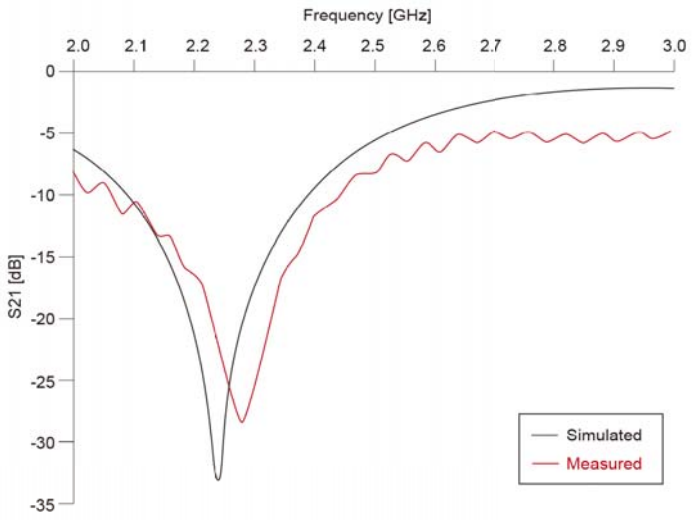

Figure 4. Measured and simulated S_{21} of the proposed sensor.

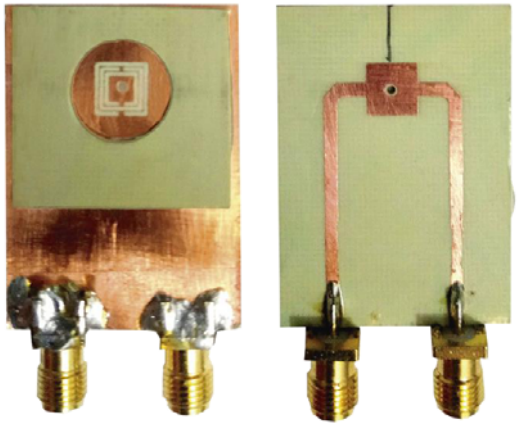

(a) sensor side (b) TL side

Figure 5. Prototype of the proposed sensor: (a) sensor side and (b) transmission line side.

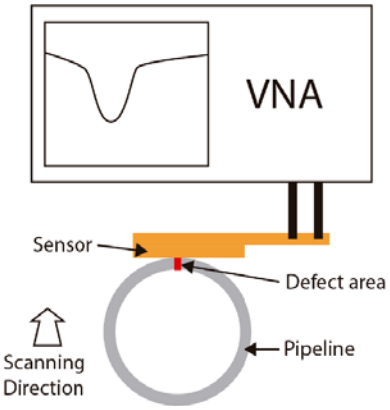

Figure 6. Diagram of test setup.

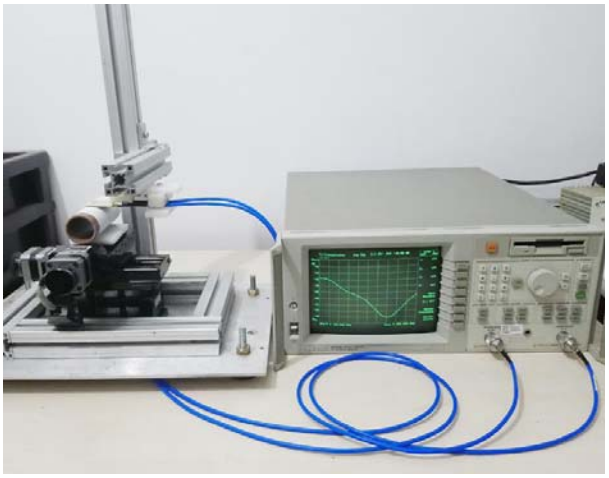

Figure 7. Complete measurement setup.

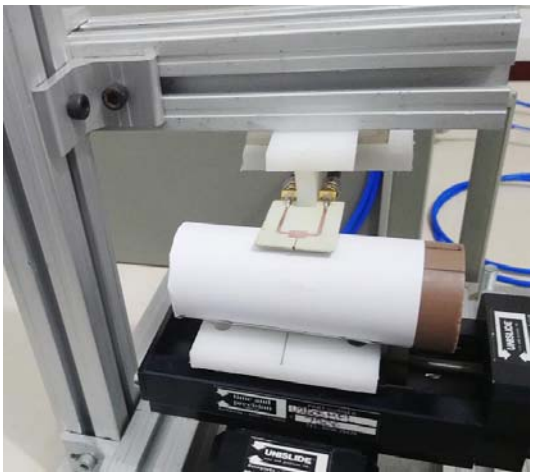

Figure 8. Details of sensor and pipeline sample in the precision XY stage.

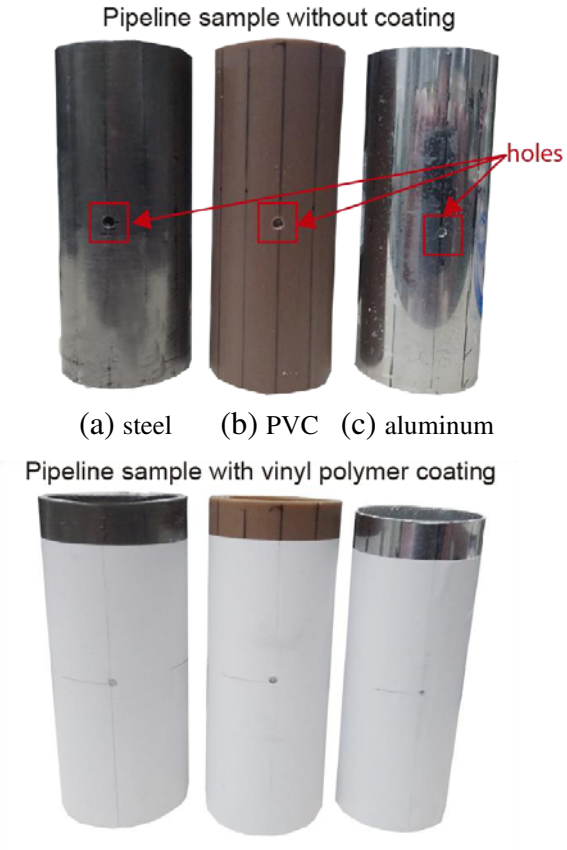

Figure 9. Pipeline samples used in measurements.

The measurement setup was built using an HP 8714B vector network analyzer (VNA) connected to the sensor to obtain the S-parameters, magnitude, and Q-factor in terms of frequency. Fig. 6 shows the diagram of the test setup.

A special support was used to hold the proposed sensor in a fixed position while the pipeline samples were moved using a precision XY stage. The whole setup can be seen in Fig. 7, and Fig. 8 shows the

details of the sensor and pipeline sample in the precision XY stage.

The pipeline samples used for the measurements are as follows: (a) steel with 42 mm outer diameter, 105 mm length, and 7.5 mm thickness; (b) PVC with 40 mm outer diameter, 105 mm length, and 2.5 mm thickness; (c) aluminum with 38.5 mm outer diameter, 105 mm length, and 1 mm thickness.

To validate the sensitivity of the sensor, three holes were drilled in each pipeline sample: 3 mm, 2 mm, and 1 mm diameters. All pipeline samples were wrapped with an adhesive vinyl polymer with 0.1 mm thickness to verify if the sensor can detect faults, even when the fault is under a coating. Fig. 9 shows the pipeline samples used in the measurements.

4. RESULTS

The transmission responses (S_{21}) were measured with a VNA, and the resonant frequency and Q-factor at each position along the line with the pipeline holes were taken.

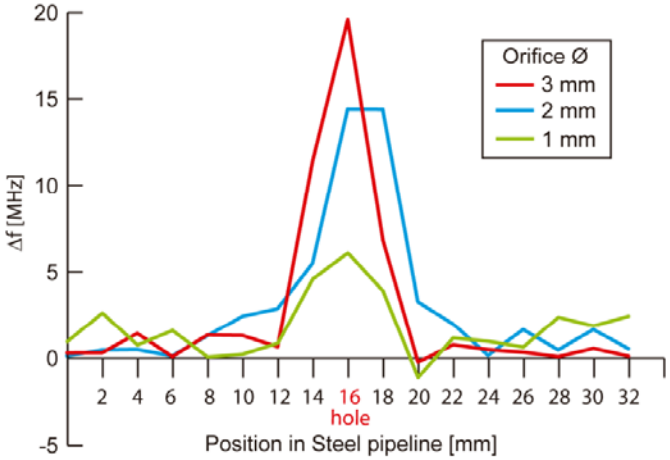

Figure 10. Frequency variation along the line with the hole in steel pipeline.

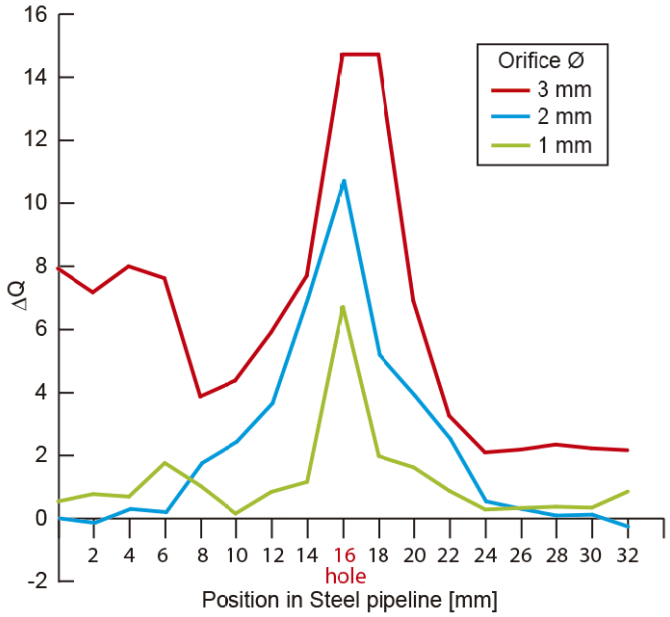

Figure 11. Q-factor variation along the line with the hole in steel pipeline.

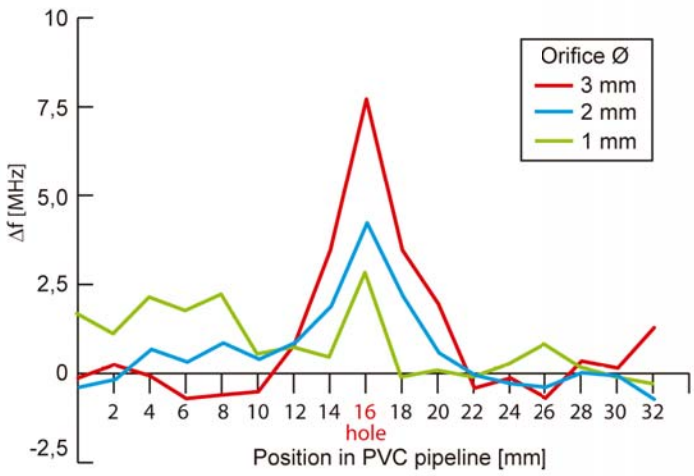

Figure 12. Frequency variation along the line with the hole in PVC pipeline.

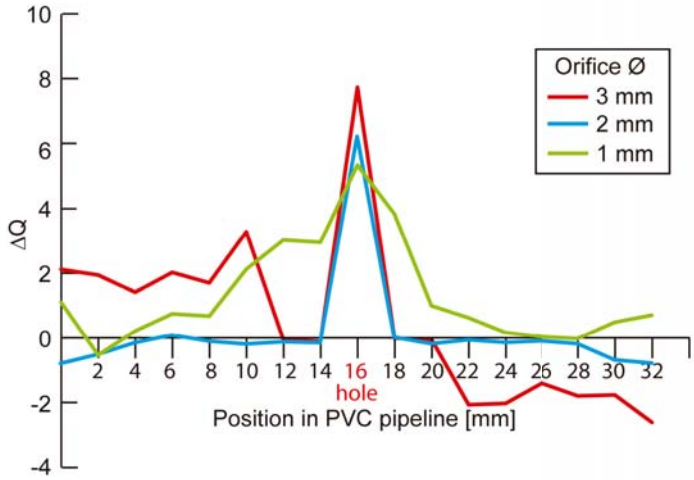

Figure 13. Q-factor variation along the line with the hole in PVC pipeline.

The resonant frequencies were observed to shift toward higher frequencies when the sensor was positioned over the holes, and the same trend occurred for the Q-factor. This shift agrees with the results predicted by numerical and simulation methods in other works [39, 40]. Figs. 10–15 show the results of the frequencies and Q-factor, which shifted as a function of the position along the line where the pipeline holes are located.

In the aluminum pipeline, the sensor presented its highest frequency variation (29.74 MHz, 24.73 MHz, and 1.70 MHz for 3 mm, 2 mm, and 1 mm holes, respectively) and Q-factor (12.58, 8.83, and 7.15 for 3 mm, 2 mm, and 1 mm holes, respectively) when positioned under the holes.

With the steel pipeline, the sensor presented a frequency variation (19.60 MHz, 14.45 MHz, and 6.10 MHz for 3 mm, 2 mm, and 1 mm holes, respectively) and Q-factor (14.77, 10.72, and 6.72 for 3 mm, 2 mm, and 1 mm holes, respectively) when positioned under the holes.

For the PVC pipeline, the sensor presented a frequency variation (7.68 MHz, 4.30 MHz, and 2.62 MHz for 3 mm, 2 mm, and 1 mm holes, respectively) and Q-factor (7.73, 6.24, and 5.18 for 3 mm, 2 mm, and 1 mm holes, respectively) when positioned under the holes.

In the resume, to the proposed sensor, the aluminum pipeline shows the maximum frequency variation, the PVC a lower frequency variation, and the steel pipeline shows an intermediate variation. The Q factor is not as variable as frequency.

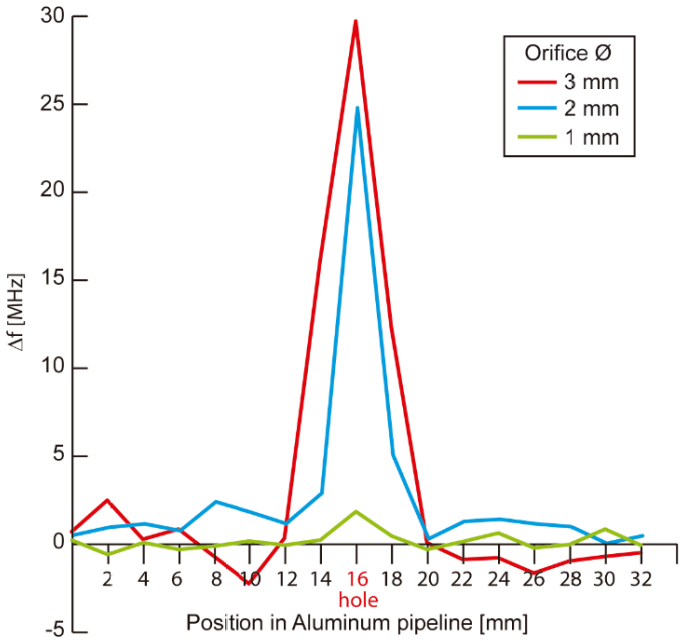

Figure 14. Frequency variation along the line with the hole in aluminum pipeline.

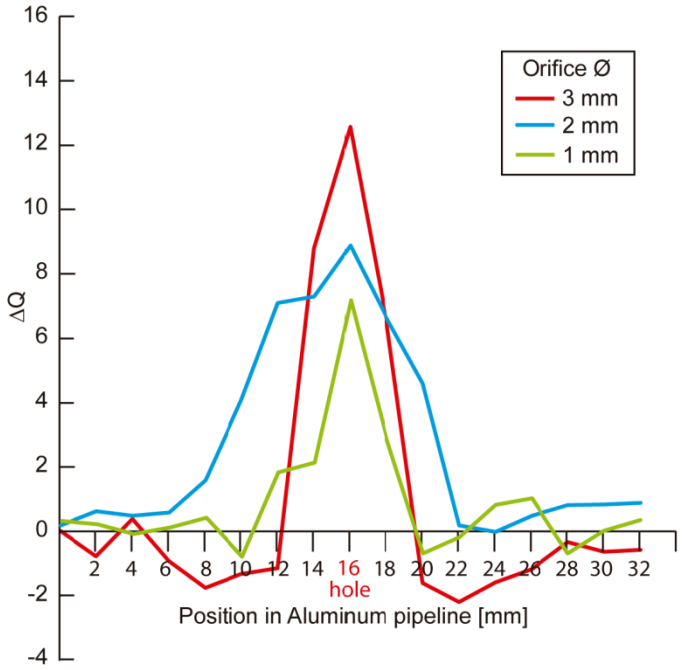

Figure 15. *Q*-factor variation along the line with the hole in aluminum pipeline.

Therefore, according to the measurements performed, the sensor can detect 1 mm faults in pipelines even when the fault is under a coating.

Other microwave sensors for crack and fault detection using CSRR were proposed in the other works [25–29]. However, the proposed sensor of this article shows an ability to detect faults in non-planar surfaces (pipeline) and even under coatings because of its new physical structure.

5. CONCLUSIONS

The sensing mechanism of the proposed CSRR microwave-based sensor is based on measuring the insertion loss (S_{21}) between two ports connected through a microstrip line, which excites the CSRR sensing element. The sensor was fabricated using inexpensive and readily available printed circuit board technology.

The proposed CSRR microwave-based sensor works in a frequency of around 2.25 GHz and can detect faults of 1 mm in pipelines of several materials even when the fault is under a coating.

The proposed sensor presents high sensitivity, small dimensions, simple design, and easy fabrication. Therefore, it is a good choice for field measurements, which is a common situation for pipeline applications.

REFERENCES

1. Mohitpour, M., *Pipeline Design and Construction: A Practical Approach*, ASME Press, 2003.
2. Boaz, L., S. Kaijage, and R. Sinde, "An overview of pipeline leak detection and location systems," *Proceedings of the 2nd Pan African International Conference on Science, Computing and Telecommunications (PACT 2014)*, 2014.
3. Jia, Z., Z. Wang, W. Sun, and Z. Li, "Pipeline leakage localization based on distributed FBG hoop strain measurements and support vector machine," *Optik*, Vol. 176, 1–13, 2019.
4. Brun, K. and R. Kurz, *Compression Machinery for Oil and Gas*, 1st Edition, Gulf Professional Publishing, 2018.
5. Adegboye, M. A., W.-K. Fung, and A. Karnik, "Recent advances in pipeline monitoring and oil leakage detection technologies: Principles and approaches," *Sensors*, Vol. 19, 2548, 2019.
6. Baroudi, U., A. A. Al-Roubaiey, and A. Devendiran, "Pipeline leak detection systems and data fusion: A survey," *IEEE Access*, Vol. 7, 97426–97439, 2019.
7. Zuo, J., et al., "Pipeline leak detection technology based on distributed optical fiber acoustic sensing system," *IEEE Access*, Vol. 8, 30789–30796, 2020.
8. Ekes, C. and B. Neducza, "Pipe condition assessments using pipe penetrating radar," *14th International Conference on Ground Penetrating Radar (GPR)*, 2012.
9. Awwad, A., et al., "Communication network for ultrasonic acoustic water leakage detectors," *IEEE Access*, Vol. 8, 29954–29964, 2020.
10. Wang, J., et al., "Novel negative pressure wave-based pipeline leak detection system using fiber Bragg grating-based pressure sensors," *Journal of Lightwave Technology*, Vol. 35, No. 16, 3366–3373, 2017.
11. Akib, A. B. M., N. B. Saad, and V. Asirvadam, "Pressure point analysis for early detection system," *IEEE 7th International Colloquium on Signal Processing and Its Applications*, 2011.
12. Stouffs, P. and M. Giot, "Pipeline leak detection based on mass balance: Importance of the packing term," *Journal of Loss Prevention in the Process Industries*, Vol. 6, No. 5, 307–312, 1993.
13. Zarifi, M. H., et al., "Microwave ring resonator-based non-contact interface sensor for oil sands applications," *Sensors and Actuators B*, Vol. 224, 632–639, 2016.
14. Karaaslan, M. and M. Bakir, "Chiral metamaterial based multifunctional sensor applications," *Progress In Electromagnetics Research*, Vol. 149, 55–67, 2014.
15. Boyarskii, D. A., V. V. Tikhonov, and N. Yu. Komarova, "Model of dielectric constant of bound water in soil for applications of microwave remote sensing," *Progress In Electromagnetics Research*, Vol. 35, 251–269, 2002.
16. Kilpijärvi, J., N. Halonen, Ja. Juuti, and J. Hannu, "Microfluidic microwave sensor for detecting saline in biological range," *Sensors*, Vol. 19, 819, 2019.
17. Mirza, A. F., C. H. See, I. M. Danjuma, et al., "An active microwave sensor for near field imaging," *IEEE Sensors Journal*, Vol. 17, No. 9, 2749–2757, 2017.

18. Baghbani, R., M. A. Rad, and A. Pourziad, "Microwave sensor for non-invasive glucose measurements design and implementation of a novel linear," *IET Wireless Sensor System*, Vol. 5, No. 2, 51–57, 2015.
19. Chen, T., S. Li, and H. Sun, "Metamaterials application in sensing," *Sensors*, Vol. 12, No. 3, 2742–2765, 2012.
20. Huang, M. and J. Yang, "Microwave sensor using metamaterials," *Wave Propagation*, 13–36, In Tech, 2011.
21. Ziolkowski, R. W. and N. Engheta, "Introduction, history, and selected topics in fundamental theories of metamaterials," *Metamaterials Physics and Engineering Explorations*, IEEE Press, John Wiley & Sons, 2006.
22. Holloway, C. L., E. F. Kuester, J. A. Gordon, et al., "An overview of the theory and applications of metasurfaces: The two-dimensional equivalents of metamaterials," *IEEE Antennas and Propagation Magazine*, Vol. 54, No. 2, 10–35, 2012.
23. Chowdhury, D. R., A. K. Azad, W. Zhang, and R. Singh, "Near field coupling in passive and active terahertz metamaterial devices," *IEEE Transactions on Terahertz Science and Technology*, Vol. 3, No. 6, 783–790, 2013.
24. Luk'yanchuk, B., N. I. Zheludev, S. A. Maier, et al., "The Fano resonance in plasmonic nanostructures and metamaterials," *Nature Materials*, Vol. 9, 707–715, 2010.
25. Albishi, A. and O. M. Ramahi, "Detection of surface and subsurface cracks in metallic and non-metallic materials using a complementary split-ring resonator," *Sensors*, Vol. 14, No. 10, 19354–19370, 2014.
26. Yun, T. and S. Lim, "High-Q and miniaturized complementary split ring resonator-loaded substrate integrated waveguide microwave sensor for crack detection in metallic materials," *Sensors and Actuators A: Physical*, Vol. 214, 25–30, 2014.
27. Albishi, A. and O. M. Ramahi, "Microwaves-based high sensitivity sensors for crack detection in metallic materials," *IEEE Transactions on Microwave Theory and Techniques*, Vol. 65, No. 5, 1864–1872, 2017.
28. Rajni, A. K. and A. Marwaha, "Complementary split ring resonator based sensor for crack detection," *International Journal of Electrical and Computer Engineering*, Vol. 5, No. 5, 1012–1017, 2015.
29. Albishi, A. M., M. S. Boybay, and O. M. Ramahi, "Complementary split-ring resonator for crack detection in metallic surfaces," *IEEE Microwave and Wireless Components Letters*, Vol. 22, No. 6, 330–332, 2012.
30. Pendry, J. B., A. J. Holden, D. J. Robbins, and W. J. Stewart, "Magnetism from conductors and enhanced nonlinear phenomena," *IEEE Transactions on Microwave Theory and Techniques*, Vol. 47, No. 11, 2075–2084, 1999.
31. Falcone, F., T. Lopetegi, J. D. Baena, et al., "Effective negative-stopband microstrip lines based on complementary split ring resonators," *IEEE Microwave and Wireless Components Letters*, Vol. 14, No. 6, 280–282, 2004.
32. Falcone, F., T. Lopetegi, M. A. G. Laso, et al., "Babinet principle applied to the design of metasurfaces and metamaterials," *Physical Review Letters*, Vol. 93, 197401, 2004.
33. Katsarakis, N., T. Koschny, M. Kafesaki, et al., "Electric coupling to the magnetic resonance of split ring resonators," *Applied Physics Letters*, Vol. 84, No. 15, 2943–2945, 2004.
34. Bilotti, F., A. Toscano, and L. Vegni, "Design of spiral and multiple split-ring resonators for the realization of miniaturized metamaterial samples," *IEEE Transactions on Antennas and Propagation*, Vol. 55, No. 8, 2258–2267, 2007.
35. Naqui, J., "Fundamentals of planar metamaterials and subwavelength resonators," *Symmetry Properties in Transmission Lines Loaded with Electrically Small Resonators*, Springer Theses book series, 2016.

36. Ansari, M. A. H., A. K. Jha, and M. J. Akhtar, "Design and application of the CSRR-based planar sensor for noninvasive measurement of complex permittivity," *IEEE Sensors Journal*, Vol. 15, No. 12, 7181–7189, 2015.
37. Bonache, J., M. Gil, I. Gil, et al., "On the electrical characteristics of complementary metamaterial resonators," *IEEE Microwave and Wireless Components Letters*, Vol. 16, No. 10, 543–545, 2006.
38. Chuma, E. L., et al., "Microwave sensor for liquid dielectric characterization based on metamaterial complementary split ring resonator," *IEEE Sensors Journal*, Vol. 18, No. 24, 9978–9983, 2018.
39. Salim, A. and S. Lim, "Complementary split-ring resonator-loaded microfluidic ethanol chemical sensor," *Sensors*, Vol. 16, 1802, 2016.
40. Chakyar, S. P., S. K. Simon, C. Bindu, J. Andrews, and V. P. Joseph, "Complex permittivity measurement using metamaterial split ring resonators," *Journal of Applied Physics*, Vol. 121, 054101-1, 2017.